UNMIXING OF LABORATORY IR SPECTRAL REFLECTANCE MEASUREMENTS OF SMOOTH PLAINS ANALOGS.

K. E. Bauch[1], A. Morlok[1], H. Hiesinger[1], M. P. Reitze[1], N. Schmedemann[1], A. N. Stojic[1], I. Weber[1], J.H. Pasckert[1], M. D'Amore[2], J. Helbert[2], A. Maturilli[2], K. Wohlfarth[3], C. Wöhler[3], [1]Institut für Planetologie (IfP), Westfälische Wilhelms-Universität Münster, Wilhelm-Klemm-Str. 10, 48149 Münster, Germany (karin-bauch@uni-muenster.de), [2]DLR-Institute for Planetary Research, Rutherfordstrasse 2, 12489 Berlin, Germany, [3]Image Analysis Group, TU Dortmund University, Otto-Hahn-Str. 4, 44227 Dortmund, Germany.

Introduction:

The Mercury Radiometer and Thermal Infrared Spectrometer (MERTIS) is part of the payload of ESA/JAXA's BepiColombo mission, launched in October 2018 [1-4]. MERTIS consists of an IR-spectrometer and radiometer, which observe the surface in the wavelength range of 7-14 µm and 7-40 µm, respectively [1,3]. This range covers several spectral features, such as the Christiansen feature, Reststrahlen bands, and Transparency feature, which allows the determination of Mercury's surface mineralogy.

MERTIS' scientific objectives [1,3] are to

a) study Mercury's surface composition,
b) identify rock-forming minerals,
c) globally map the surface mineralogy, and
d) study surface temperature and thermal inertia.

During its cruise to Mercury, the spacecraft has already completed four swing-by maneuvers at Earth/Moon (2020), Venus (2020&2021), and Mercury (2021). In the following years it will perform further swing-by maneuvers at Mercury [4].

During the first swing-by maneuvers MERTIS acquired thermal infrared spectra of the lunar surface and Venus. Thus, these flybys offered the first opportunity to test the instrument under 'real' planetary observation conditions [4,6].

MERTIS will be the first instrument to observe the surface of Mercury in the IR wavelength range [3]. The current knowledge of IR spectroscopy of Mercury is based on terrestrial telescopic observations [7]. The surface rocks are composed of a variety of different minerals. The ~500 m pixel size of MERTIS will therefore depict a mixture of these minerals. In order to quantify the mineral abundances, we use a non-linear unmixing model, based on the Hapke reflectance model [8,9]. The intrinsic reflectivity of an average single surface is described by the "single-scattering albedo" [8]. Multiple scattering within a surface is governed by the incidence and emission angle, which also depends non-linearly on the single-scattering albedo. The scattering behavior of an individual particle is described by a "single-particle scattering function". The full set of equations is provided by [8].

The unmixing model used in this study has previously been used for spectral unmixing of NASA RELAB data [10] and lunar analog materials [11]. In the framework of MERTIS it is applied to laboratory mineral mixtures, including glasses and varying grain sizes [12-14].

These mixtures are prepared and analyzed at the IRIS (Infrared and Raman for Interplanetary Spectroscopy) laboratory of the Institut für Planetologie at the Westfälische Wilhelms-Universität Münster [3]. Here we investigate a wide range of natural minerals, rock samples including impact rocks and meteorites, synthetic analogs, and glasses [3,7]. The results of these investigations contribute to the generation of a mid-IR reflectance database in the MERTIS-relevant wavelength range from 7-14 µm. This database enables the qualitative, but also quantitative interpretation of MERTIS spectra.

IR spectroscopy:

At the IRIS laboratory, samples are sieved in grain size fractions smaller 25 µm, 25 to 63 µm, 63 to 125 µm, and 125 to 250 µm. For the mineral mixing analysis presented here, we focus on the 63-125 µm grain size fraction. Samples are placed in aluminum cups and analyzed by a Bruker Vertex 70v infrared system. The use of an A513 variable mirror reflectance stage allows for variations in orbital geometry. Here we focus on the 20° incidence (i) and 30° emergent (e) angle measurements. After background calibration using a commercial diffuse gold standard (INFRAGOLD™) a total of 512 scans for each analysis were integrated to ensure high signal-to-noise ratios [6].

Samples:

Studies by [15-17] suggest that the surface of Mercury is dominated by plagioclase, forsterite, diopside, enstatite, and quartz, but also constists of unconstrained proportions of silicate glasses. Hence, for the present study, we analyzed mixtures using the following samples:

- ID22 diopside from Otter Lake, Quebec,
- ID28 labradorite from Ihosy, Madagascar,
- ID53 enstatite from Bamble, Norway,
- ID249 olivine from Dreyser Weiher, Germany.
- ID158 synthetic low Mg B glass, and
- ID174 synthetic low Mg A II glass.

IDs refer to the identifiers in our database. The glasses are based on compositions of low Mg smooth plain regions [17], a detailed description is given by [7]. From these endmembers, we derived different mineral mixtures, based on studies of smooth plain regions on Mercury, which were analyzed by the unmixing model.

Results:

Reflectance spectra of the endmembers and their mixtures are shown in Figure 1 for different grain size fractions. The samples ID22 diopside, ID28 labradorite, enstatite, and ID249 olivine show characteristic Christiansen features (CF) and Reststrahlen bands (RB). Low Mg B (ID158) has the CF at 7.8 µm and a single RB at 9.4 µm. For low Mg A II (ID174) the CF and RB are at 7.9 µm and 9.6 µm, respectively. Due to the large amount of glasses in the mixtures, their corresponding reflectance spectra are relatively flat and characteristic features are shifted due to the glassy component. This is especially visible in all grain size fractions for ID345 (Mix 3), which consists of only two endmembers with a very high glass amount (>90%).

Results of the spectral unmixing procedure of the mixtures are summarized in Table 1.

Table 1 Spectral unmixing results of smooth-plains-glass mixtures. Actual fractions of the mixtures are written in italics.

	ID343		ID344		ID345	
	actual	comp.	*actual*	comp.	*actual*	comp.
ID22 Diopside	*10.8%*	10.0%	*2.0%*	2.1%		
ID28 Labradorite	*33.8%*	39.0%	*27.1%*	22.8%		
ID53 Enstatite	*7.1%*	7.5%	*11.4%*	10.4%		
ID249 Olivine	*6.1%*	6.4%	*5.0%*	4.6%	*9.1%*	10.7%
ID158 Low Mg B	*42.2%*	37.1%	*54.5%*	60.1%		
ID174 Low Mg A II					*90.9%*	89.4%

Summary & Conclusions:

Quantitative results of spectral unmixing of glass mixtures show good overall agreement with the actual proportions. The minerals with very distinct spectral features (ID249 olivine, ID53 enstatite, and ID22 diopside) are computed with only little deviation (~1%) from the actual fractions for mixtures ID343 and ID344.

However, the computed proportion of ID28 labradorite and both glasses show larger deviations (~5%) from the actual fractions due to their rather flat spectra with less pronounced characteristic features. This is also in agreement with previous studies [14] of labradorite-enstatite-glass mineral mixtures, where the enstatite fraction could be determined very precisely, while computed labradorite and glass fractions deviate from the actual proportions (~5%).

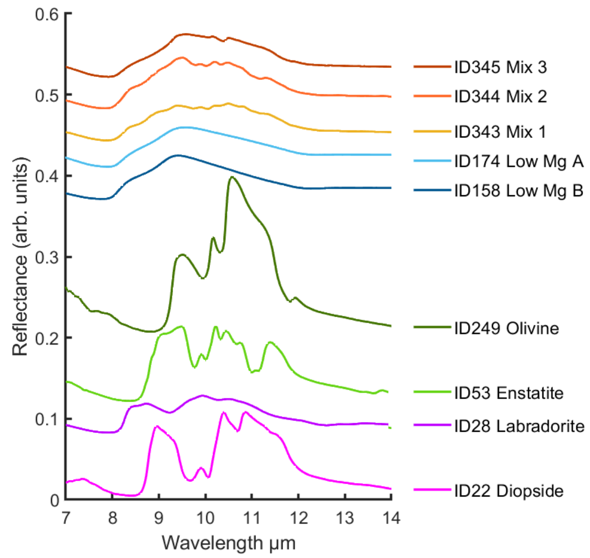

Figure 1 IR reflectance spectra of endmembers and synthetic smooth plain mixtures in the MERTIS-relevant wavelength range between 7-14 µm for 20°(i)/30°(e) for the grain size fraction 63-125µm.

These results show that further studies of mineral mixtures including more components and varying amounts of glasses are needed.

With ongoing calibration of MERTIS data, our unmixing routine can also be applied to quantitatively interpret the spectra from the past lunar and hopefully also further swing-by maneuvers at Mercury and finally orbital measurements, starting in 2026.

Acknowledgements:

This work was supported by DLR grant 50 QW 1302/1701 in the framework of the BepiColombo mission (K.E.B., A.M., M.P.R., A.N.S., I.W.).

References: [1] Hiesinger H. et al. (2010) *PSS 58,* 144-165. [2] Benkhoff J. et al. (2010) *PSS 58,* 2-20. [3] Hiesinger et al. (2020) *Space Sci Rev. 216,* 8, id.147. [4] Benkhoff, J. et al. (2021) *Space Sci Rev.* 217, 8, id.90. [5] Maturilli, A. et al. (2021) *LPSC LII*, 1435. [6] Hiesinger, H. et al. (2021) *LPSC LII*, Abstract #1494. [7] Morlok, A. et al. (2020) *Icarus335,* 113410. [8] Hapke B. (1981), *JGR 86(B4),* 3039-3054. [9] Mustard, J.F. and Pieters, C.M. (1987) *JGR 92(B4)*, E617–E626. [10] Grumpe A. et al (2017) *Icarus 299,* 1-14. [11] Rommel D. et al. (2017) *Icarus 284,* 126-149. [12] Bauch, K.E. et al. (2019) *LPSC L,* Abstract #2521. [13] Bauch, K.E. et al. (2020) *LPSC LI,* Abstract #1523. [14] Bauch, K.E. et al. (2021) *LPSC LII,* Abstract 1567. [15] Charlier, B. et al. (2013) *EPSL 363,* 50-6. [16] Namur, O. et al. (2016) *EPSL 439,* 117-128. [17] Namur O. and Charlier, B. (2017) *NGEO 10,* 9-13.